Original Article

CDK12 inhibition enhances oxaliplatin efficacy in gastric cancer by suppressing the MAPK signaling pathway

Dayin Huang[1,2,3#], Zhizhong Xiong[1,2,3#], Bin Zhong[1,2,3#], Xianwen Li[4,5], Saddam Ahmed Mohamed[1,2,3], Jiachen Sun[1,6], Haoyang Xu[1,2,3], Jianping Guo[1,2,3,7], Zijian Deng[1,2,3], Xianzhe Li[8], Khaldoun Almhanna[9], Yonghe Chen[1,2,3], Lei Lian[1,2,3]

[1]Department of General Surgery (Department of Gastrointestinal Surgery), The Sixth Affiliated Hospital, Sun Yat-sen University, Guangzhou, China; [2]Guangdong Provincial Key Laboratory of Colorectal and Pelvic Floor Diseases, The Sixth Affiliated Hospital, Sun Yat-sen University, Guangzhou, China; [3]Biomedical Innovation Center, The Sixth Affiliated Hospital, Sun Yat-sen University, Guangzhou, China; [4]State Key Laboratory of Respiratory Disease, The First Affiliated Hospital of Guangzhou Medical University, Guangzhou Medical University, Guangzhou, China; [5]Guangzhou National Laboratory, Guangzhou, China; [6]Department of Gastrointestinal Endoscopy, The Sixth Affiliated Hospital, Sun Yat-sen University, Guangzhou, China; [7]Key Laboratory of Immune Response and Immunotherapy, China-New Zealand Joint Laboratory of Biomedicine and Health, Guangdong Provincial Key Laboratory of Biocomputing, Institute of Drug Discovery, Guangzhou Institutes of Biomedicine and Health, Chinese Academy of Sciences, Guangzhou, China; [8]Division of Clinical Epidemiology and Aging Research, German Cancer Research Center (DKFZ), Heidelberg, Germany; [9]Division of Hematology/Oncology, The Warren Alpert Medical School of Brown University, Rhode Island Hospital, Providence, RI, USA

Contributions: (I) Conception and design: D Huang, L Lian; (II) Administrative support: L Lian; (III) Provision of study materials or patients: Y Chen, L Lian; (IV) Collection and assembly of data: D Huang, Z Xiong, B Zhong, Xianwen Li, SA Mohamed, J Sun, L Lian; (V) Data analysis and interpretation: D Huang, Z Xiong, B Zhong, Xianwen Li, H Xu, L Lian; (VI) Manuscript writing: All authors; (VII) Final approval of manuscript: All authors.

[#]These authors contributed equally to this work as co-first authors.

Correspondence to: Yonghe Chen, MD; Lei Lian, MD, PhD. Department of General Surgery (Department of Gastrointestinal Surgery), The Sixth Affiliated Hospital, Sun Yat-sen University, 26 Yuancun Er Heng Rd., Guangzhou 510655, China; Guangdong Provincial Key Laboratory of Colorectal and Pelvic Floor Diseases, The Sixth Affiliated Hospital, Sun Yat-sen University, Guangzhou, China; Biomedical Innovation Center, The Sixth Affiliated Hospital, Sun Yat-sen University, Guangzhou, China. Email: chenyhe@mail2.sysu.edu.cn; lianlei2@mail.sysu.edu.cn.

Background: Gastric cancer (GC) is a leading cause of cancer-related mortality worldwide. Oxaliplatin (OXA) based therapy plus/minus targeted therapy and immune check point inhibitors is the standard first-line treatment for advanced GC; however, its clinical efficacy is often hindered by the development of drug resistance. Cyclin-dependent kinase 12 (CDK12), a transcriptional regulator linked to DNA repair, plays a crucial role in transcription, cancer progression as well as drug resistance, where its exact role is unclear. In this study, we will investigate the role of CDK12 in GC progression and its potential as a therapeutic target specifically to enhance the efficacy of OXA.

Methods: CDK12 expression in GC tissues was analyzed by quantitative polymerase chain reaction (qPCR) and tissue microarrays (TMAs). A Kaplan-Meier survival analysis was conducted to assess the relationship between CDK12 levels and clinical outcomes. The effect of the CDK12 inhibitor combined with OXA was evaluated through *in vivo* and *in vitro* models. RNA-sequencing and western blots were used to investigate the molecular mechanisms of CDK12 inhibitor sensitizing OXA.

Results: CDK12 exhibited significant amplification frequency in GC. The Mendelian-randomization analysis revealed a positive causal association between elevated CDK12 expression and an increased risk of GC. Additionally, CDK12 was significantly overexpressed in GC tissues compared with adjacent normal tissues, and its high expression was significantly associated with a worse prognosis. The functional assays revealed that combining the CDK12 inhibitor THZ531 with OXA synergistically suppressed GC cell proliferation, induced apoptosis, and reduced colony formation *in vitro*, while substantially inhibiting tumor growth in xenograft models. Mechanistically, CDK12 inhibition disrupted MAPK signaling, leading to enhanced OXA-induced DNA damage and potentiated anti-tumor effects.

Conclusions: Our findings suggest that CDK12 inhibition may represent a promising strategy for overcoming OXA resistance and improving GC treatment outcomes.

Keywords: Gastric cancer (GC); cell cycle; cyclin-dependent kinase 12 (CDK12); combination therapy; oxaliplatin (OXA)

Submitted May 19, 2025. Accepted for publication Jun 10, 2025. Published online Jun 23, 2025.
doi: 10.21037/jgo-2025-392
View this article at: https://dx.doi.org/10.21037/jgo-2025-392

Introduction

Gastric cancer (GC) remains a significant global health problem, it is one of the most common malignancy worldwide. In 2022, there were 968,400 new cases of GC, making it the fifth most common cancer worldwide, and 659,900 GC-related deaths, making it the fifth leading cause of cancer-related deaths worldwide (1). GC is particularly prevalent in China and poses a significant public health challenge (2). Due to atypical and occult symptoms in the early stages, most GC patients are diagnosed at advanced stages which impact prognosis as the cancer has spread beyond the stomach at the time of diagnosis (3). Oxaliplatin (OXA)-based combination chemotherapy plus/minus targeted therapy and immune checkpoint inhibitors remains the standard first-line standard treatment for advanced GC, offering survival benefits and disease control (4). However, chemoresistance remains a significant challenge affecting overall survival (5). Understanding and overcoming the molecular mechanism behind chemoresistance is crucial for improving treatment outcome in patients with GC.

OXA resistance is a major clinical challenge and is closely associated with dysregulated cell-cycle progression and enhanced DNA damage repair mechanisms (6,7). Cyclin-dependent kinases (CDKs), key regulators of the cell cycle, play significant role in OXA resistance, thus, CDK inhibitors may be a potential therapeutic strategy to overcome the resistance (8,9). The CDK family comprises 20 members (CDK1–20). Notably, cyclin-dependent kinase 12 (CDK12) plays critical roles in DNA repair, including cell-cycle regulation, transcription, and the DNA damage response (10). CDK12 mutations and amplifications is the predominant alteration in cancer (11,12). Therefore, understanding and targeting the CDK12 in GC can restore sensitivity to oxaliplatin and enhance its anti-tumor effects.

Multiple CDK inhibitors have been designed as potential therapeutic agents for the treatment of cancer (13,14) and more recently CDK12 inhibitors (15). The inhibition of CDK12 has shown promise in preclinical models, particularly in enhancing the sensitivity of prostate cancer to chemotherapy and targeted therapies (16). Recent studies suggest that CDK12 inhibitors can also sensitize breast cancer to DNA-damaging agents by impairing DNA repair mechanisms (17,18). These findings suggest that CDK12 inhibitors may potentiate the efficacy of chemotherapeutic agents in tumors characterized by enhanced DNA repair capacity. However, the question of whether CDK12 inhibition can overcome chemoresistance in GC remains

Highlight box

Key findings

- Cyclin-dependent kinase 12 (CDK12) is overexpressed in gastric cancer (GC) tissues and is associated with poor survival outcomes.
- CDK12 inhibition using THZ531 enhances oxaliplatin (OXA)-induced DNA damage and apoptosis *in vitro* and *in vivo*.
- The synergistic effect of THZ531 and OXA is mediated by the suppression of the MAPK signaling pathway.

What is known, and what is new?

- OXA-based chemotherapy plus/minus targeted therapy is the standard first-line treatment for advanced GC, but its efficacy is often hindered by the development of resistance. CDK12 is a transcription-associated cyclin-dependent kinase involved in DNA damage repair and has been implicated in drug resistance in several cancers.
- Our findings suggest that CDK12 could serve as a prognostic biomarker and a therapeutic target for GC. Further, we found that CDK12 inhibition sensitizes GC cells to OXA by amplifying DNA damage and impairing MAPK signaling.

What is the implication, and what should change now?

- Targeting CDK12 is a promising therapeutic strategy to overcome OXA resistance in GC.
- Combining CDK12 inhibitors with DNA damaging agents like OXA can become a novel therapeutic approach for the treatment of advanced GC.
- Future clinical studies should evaluate the safety and effectiveness of CDK12-targeted therapies in OXA-resistant GC patients.

largely unexplored. Given the pivotal role of CDK12 in DNA damage repair and its association with chemotherapy resistance, further studies are needed to evaluate the ability of CDK12 inhibitors to restore OXA sensitivity and improve therapeutic outcomes in GC.

This study aim is to explore the role and the mechanisms of CDK12 in GC progression and chemoresistance and evaluate the potential of CDK12 inhibition to enhance DNA damage and overcome OXA resistance. We present this article in accordance with the ARRIVE and MDAR reporting checklists (available at https://jgo.amegroups.com/article/view/10.21037/jgo-2025-392/rc).

Methods

Clinical samples and tissue microarrays (TMAs)

Twenty paired gastric cancer and adjacent normal tissues were freshly collected from patients undergoing radical gastrectomy at The Sixth Affiliated Hospital of Sun Yat-sen University. The study was conducted in accordance with the Declaration of Helsinki and its subsequent amendments. The study was approved by the Research Ethics Board at The Sixth Affiliated Hospital of Sun Yat-sen University (No. 2025ZSLYEC-047) and informed consent was taken from all the patients.

Paraffin-embedded samples from 324 GC patients undergoing initial radical resection between January 2013 and August 2022 were evaluated. Comprehensive clinicopathological data, including tumor staging (using the American Joint Committee on Cancer criteria), were obtained from the GC database. Tumor tissue cores were obtained from representative areas and embedded into TMAs for further analysis. Immunohistochemical (IHC) staining was conducted on 5-μm slices, followed by antigen retrieval and staining with primary antibodies.

Evaluation of IHC analysis

IHC staining was assessed using a semi-quantitative scoring methodology in accordance with protocols described in previous study (19). Two trained researchers assigned an intensity score to each TMA spot, ranging from 1 (the weakest) to 4 (the strongest). The proportion of positively stained cancer cells was quantified in 25% increments (≤25% =1, 26–50% =2, 51–75% =3, >75% =4), and the final H-score was calculated as the product of these two components (intensity score × percentage score). Statistical analysis was conducted using GraphPad Prism software (version 8.3.1).

For the hematoxylin and eosin staining, the tumor tissues were fixed in 4% formalin, embedded in paraffin, and sectioned into 5-μm slices. Following deparaffinization and rehydration, the antigen was retrieved by being microwaved in ethylenediaminetetraacetic acid (EDTA) buffer. Endogenous peroxidase was then blocked with 3% hydrogen peroxide and then incubated with goat serum for 1 hour. Next, the sections were incubated overnight at 4 ℃ with primary antibodies against CDK12 (1:500, Abcam, Cambridge, UK, ab317746), Ki-67 (1:400, CST, Boston, USA, #9449), and cleaved-caspase 3 (1:200, CST, Boston, USA, #9661). Afterward, a secondary antibody was applied for 20 minutes. Immunostaining was then visualized using diaminobenzidine, and the slices were counterstained with hematoxylin.

Differential expression analysis

RNA-sequencing data from The Cancer Genome Atlas (TCGA) (https://portal.gdc.cancer.gov/) and Genotype-Tissue Expression (GTEx) databases (http://gtexportal.org/home/) were used to identify the differentially expressed genes (DEGs) and pathways. A Kyoto Encyclopedia of Genes and Genomes (KEGG) pathway analysis and a gene set enrichment analysis (GSEA) were performed using the limma (Bioconductor) and ClusterProfiler (Bioconductor) packages of R software (version 4.3.2). The criteria for differential expression were set as follows: "adjusted $P<0.05$ and $Log_2 >1$". The GSEA results are presented as normalized enrichment scores. A false discovery rate of <0.25 and a P value <0.05 were set as the thresholds for determining statistical significance.

Potential target genes of GC

The data for the cell cycle-associated target genes were obtained from the Genecards database (https://www.genecards.org/, Weizmann Institute of Science), which is a comprehensive platform that provides detailed predictions and annotations of human genes (20). The GeneCards database was searched for enriched DEG pathways by targeting the top 1,000 genes or using a minimum score threshold of 7. Potential genes targeting cell-cycle regulation came from the CDK family (13,21,22). The table available at https://cdn.amegroups.cn/static/public/jgo-2025-392-1.xlsx provides detailed information on

the identified cell cycle-related target genes and their corresponding pathway annotations. A Venn diagram (https://bioinformatics.psb.ugent.be/webtools/Venn/) was generated to visualize the overlapping DEGs among the five cell-cycle pathways.

Two-sample Mendelian randomization (MR)

This study employed two-sample MR to assess the causal relationship between CDK12 and GC. The inverse variance-weighted (IVW) method, known for its high statistical power, was the primary analytical method for assessing effect estimates when two or more instrumental variables (IVs) were present. Four additional two-sample MR analysis methods (i.e., Egger, weighted median, simple mode, and weighted mode) were used to supplement the IVW results. Sensitivity analyses, such as MR-Egger regression and MR-Pleiotropy RESidual Sum and Outlier analyses, were conducted to evaluate horizontal pleiotropy and ensure robustness. Cochran's *Q* test was used to quantify the heterogeneity among the IVs, while a leave-one-out analysis was conducted to assess the influence of individual single nucleotide polymorphisms (SNPs). Odds ratios (ORs) and 95% confidence intervals (CIs) were used to present all the results. A P value <0.05 was considered statistically significant. The genetic variants for CDK12 and GC were obtained from the IEU Open GWAS Project (https://gwas.mrcieu.ac.uk/). The CDK12 genetic data were obtained from the project eQTL dataset in IEU Open GWAS, and the outcome GWAS identification was "finn-b-C3_STOMACH". In this study, IVs were selected based on the following criteria: $P<5\times10^{-8}$, or $P<1\times10^{-5}$ when there were not enough genome-wide significant loci. Notably, linkage disequilibrium was managed by clumping to minimize bias; and IVs with an *F*-statistic <10 were omitted to alleviate weak instrument bias.

Kaplan-Meier (K-M) survival analysis

We study the correlation between CDK12 expression and overall survival in patients with GC using K-M plotter (https://kmplot.com/).

RNA sequencing

The sequencing of messenger RNAs (mRNAs) was performed on the DNBSEQ platform (BGI Co., Ltd., Beijing, China) to identify the differentially expressed mRNAs within paired GC tissues.

Cell culture and treatment

All the commercial cell lines were obtained from American Type Culture Collection (ATCC). All human gastric cell lines (GES-1, AGS, NCI-N87, SNU638, SNU668, NUGC3, NUGC4 and HGC27) were maintained in Roswell Park Memorial Institute Medium 1640 or Dulbecco's Modified Eagle Medium supplemented with 1% penicillin/streptomycin (Gibco, CA, USA) and 10% fetal bovine serum (HyClone, GE Healthcare Life Sciences, Pittsburgh, PA, USA). THZ531 (T4293), a potent CDK12 and CDK13 inhibitor, was purchased from Targetmol (Boston, MA, USA).

Colony formation assay

Single-cell suspensions were seeded at a density of 20,000 cells per well in six-well plates. The medium was replaced every 3 days during the 12-day culture period. The cell colonies were then fixed, stained and photographed.

Cell proliferative assay

To examine growth inhibition, the cells were plated in black 96-well microtiter plates at the optimal seeding density, with three replicates per condition. After 24 hours, the cells were treated with either OXA THZ531, or a combination of both, and cultured at 37 ℃ for 96 hours. The CellTiter-Glo Luminescent Cell Viability Assay (#G7573, Promega, Madison, WI, USA) was performed following procedures described in the product instructions.

Tumorsphere formation assay

First, 10,000 cells were evenly seeded into each well of a 12-well ultra-low attachment plate, which was supplemented with heparin (1:500), hydrocortisone (0.5 μg/mL), and Mammocult medium (STEMCELL Technologies, Vancouver, BC, Canada). To maintain the integrity of the tumor spheres, 500 mL of the same medium were replenished tri-daily. After a 10-day incubation period, the spheres were photographed and subjected to semi-quantitative analysis using ImageJ software (version 2.0.0).

Reverse transcription-qPCR

Total RNA was isolated using TRIZOL (Invitrogen,

Karlsruhe, Germany) and then reverse-transcribed with ReverTra Ace® quantitative polymerase chain reaction (qPCR) reverse transcription (RT) Master Mix (TOYOBO, Osaka, Japan). Gene expression was measured using the LightCycler480 PCR system (Roche, Mannheim, Germany) using 2× SYBR Green qPCR Master Mix (Biotool, Texas, USA, #B21203) and normalized to glyceraldehyde-3-phosphate dehydrogenase (GAPDH). The following primer sequences were used: CDK12-F: 5'-ACCCTACAGAGCGACTTCCTTAAA-3' and CDK12-R: 5'-TTCGAGAAGTTTTGGATGGAGGTG-3', GAPDH-F: 5'-GGAGCGAGATCCCTCCAAAAT-3' and GAPDH-R: 5'-GGCTGTTGTCATACTTCTCATGG-3'.

Western blot analysis

Protein extracts were prepared with radioimmunoprecipitation assay (RIPA) cell lysis buffer (containing 1 mM of EDTA, 50 mM of Tris-HCl, 150 mM of NaCl, 200 mM of NaF, and 200 mM of phenylmethanesulfonyl fluoride (PMSF), 0.5% deoxycholate sodium, and 1.0% NP40), and the protease inhibitor cocktail (Roche, Basel, Switzerland). The protein samples were analyzed by sodium dodecyl sulfate-polyacrylamide gel electrophoresis, transferred to polyvinylidene fluoride membranes, and subjected to immunoblotting. The primary antibodies used were anti-CDK12 rabbit mAb (#11973S, CST, Boston, USA) and anti-GAPDH mouse mAb (#GB12002-100, Servicebio, Wuhan, China).

Xenograft tumor model in nude mice

To establish the xenograft tumor model, 5×10^6 NUGC3 cells suspended in 0.1 mL of phosphate-buffered saline were subcutaneously injected into the right flank of female athymic BALB/c nude mice (5–8 weeks old, purchased from GemPharmatech, Nanjing, China). The tumor-bearing mice were housed under specific pathogen-free conditions with a controlled temperature and light cycles. When the tumors reached an average volume of 70 mm^3, the mice were randomized into the following four groups (n=4/group) with matched tumor burdens: the control group, which received an intraperitoneal (i.p.) injection of dimethyl sulfoxide (DMSO); the THZ531 monotherapy group, which received 10 $mg{\cdot}kg^{-1}$ every 3 days (i.p.); the OXA monotherapy group, which received 3 mg kg^{-1} every 3 days (i.p.); and the combination therapy group, which received THZ531 + OXA (at the same doses and schedule as the monotherapy and i.p. injection groups). The tumor volume and whole-body weight were measured every other day using Vernier calipers, and the volume was calculated using the following formula: $V = W^2 \times L/2$. Therapeutic efficacy was evaluated over ~3 weeks post-treatment initiation. The mice were euthanized when the tumors reached 1,000 mm^3 or at the conclusion of the study. The excised tumors were weighed, photographed, and preserved for downstream analyses. A protocol was prepared before the study without registration. All the animal experiments were performed under a project license (No. IACUC-2023080302) granted by the Laboratory Animal Ethics Committee of The Sixth Affiliated Hospital of Sun Yat-sen University, in compliance with institutional guidelines for the care and use of animals.

Statistical analysis

The data are expressed as the mean ± standard deviation, unless otherwise specified. Statistical significance was assessed using a two-tailed Student's *t*-test for comparisons between two groups, and a two-way analysis of variance with Dunnett's multiple comparisons test for analyses of multiple groups, using GraphPad Prism software (version 8.3.1). A P value <0.05 was considered statistically significant.

Results

Cell-cycle pathway dysfunction is a critical characteristic of GC

To identify potential targets in the pathogenesis and progression of GC, the DEGs in the paired tumor and adjacent non-tumor tissues from GC patients were analyzed. The KEGG pathway enrichment analysis revealed significant enrichment of the cell-cycle pathway and other pathways related to cell-cycle regulation in the GC tissues compared to their non-tumorous counterparts (*Figure 1A*). Given the central role of the CDK family in regulating the cell cycle (23), we examined the CDK family along with cell cycle–related pathways from the GeneCards database. The Venn diagram analysis revealed that CDK1, CDK2, CDK4, CDK7, CDK9, and CDK12 were significantly involved as key mediators in the cell cycle (*Figure 1B*). Notably, CDK12 showed the most significant genomic alterations in TCGA-GC dataset (*Figure 1C*). CDK12 was primarily characterized by a high frequency of amplification, which likely contributes to its overexpression and subsequent effect on cell-cycle dysregulation. Moreover, an examination

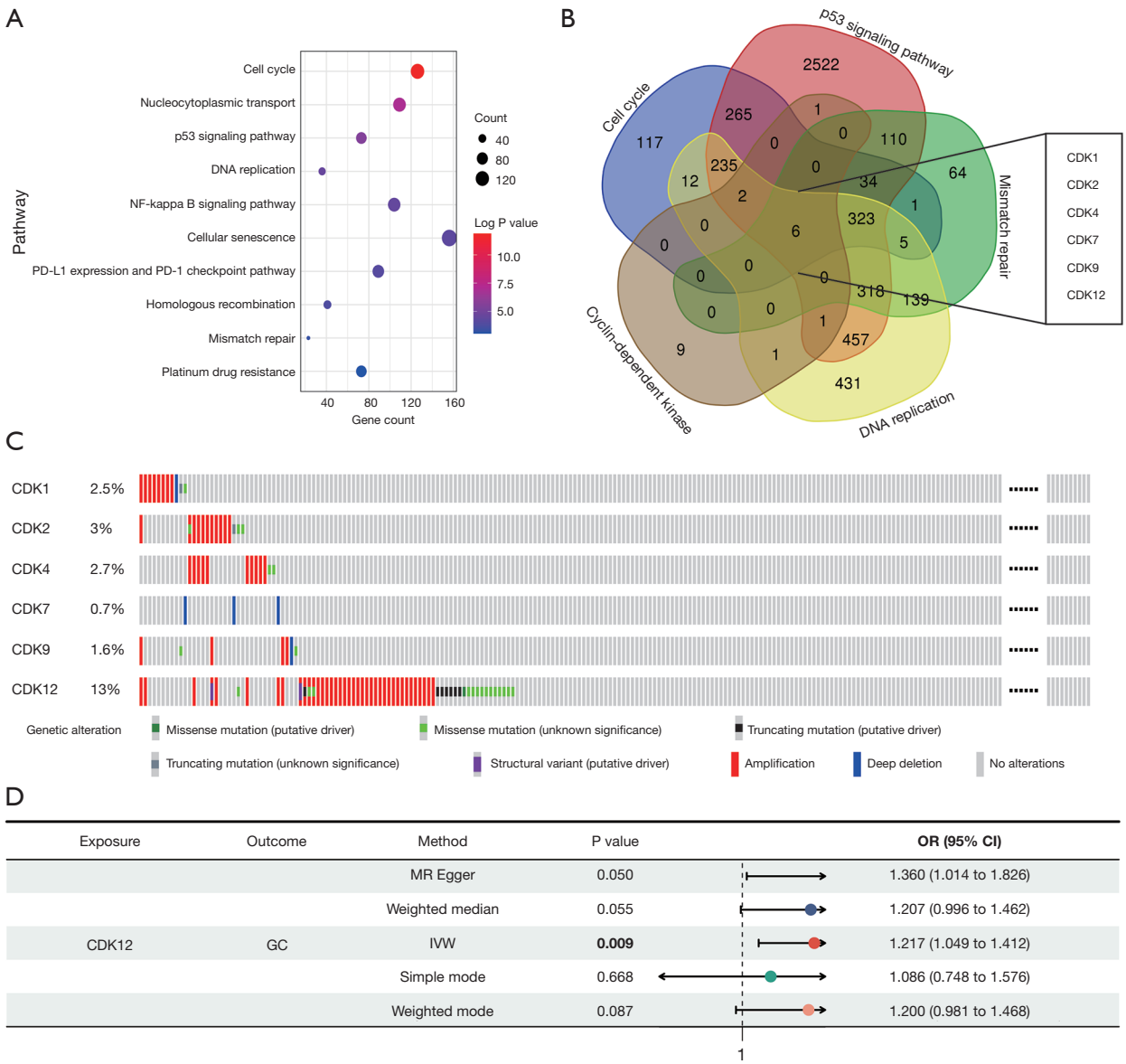

Figure 1 Cell-cycle pathway dysfunction is a critical characteristic of GC. (A) Functional enrichment: enriched KEGG signaling pathways in GC tissues compared to adjacent non-tumor tissues. (B) Venn diagram analysis illustrating the overlap between the cell cycle-related pathways from the KEGG and CDK family members derived from the GeneCards database. (C) Distribution of genomic alterations in the CDKs in TCGA-GC cohort. (D) Associations between CDK12 expression and GC based on MR analysis. CDK12, cyclin-dependent kinase 12; CI, confidence interval; GC, gastric cancer; IVW, inverse variance weighted; KEGG, Kyoto Encyclopedia of Genes and Genomes; MR, Mendelian randomization; OR, odds ratio; PD-1, programmed cell death 1; PD-L1, programmed death-ligand 1; TCGA, The Cancer Genome Atlas.

of CDK12 alterations across 32 cancer types showed that GC had the highest mutation rate for CDK12 (Figure S1). A two-sample MR analysis showed that increased CDK12 expression correlates with an increased risk of GC (OR =1.217, 95% CI: 1.049–1.412), representing a 21.7% increase in the risk of GC for every standard deviation increase in CDK12 expression (*Figure 1D*). The sensitivity analysis results revealed no pleiotropy and heterogeneity (Figure S2 and Tables S1,S2). These results highlight the critical function of CDK12 in GC development, confirming

its potential as a significant therapeutic target.

CDK12 is increased in tumor tissues and correlates with poor prognosis

To explore the clinical significance of CDK12 in GC, we initially examined the RNA-sequencing data from TCGA-stomach adenocarcinoma (STAD) cohort, which showed that the CDK12 mRNA expression was significantly increased in the tumor tissues relative to the adjacent normal tissue (*Figure 2A*). The K-M survival analysis revealed a significant association between high CDK12 expression and shorter OS (*Figure 2B*), indicating CDK12's potential as a prognostic biomarker. Findings were similar in our cohort of 20 GC patients where CDK12 mRNA levels were higher in tumor tissues compared to their normal counterparts (*Figure 2C*). We further substantiated these findings through comprehensive IHC profiling on TMAs that included 324 GC cases with detailed clinicopathological annotations (*Table 1*). CDK12 was significantly upregulated in the GC tissues relative to the corresponding normal gastric tissues (*Figure 2D*). Patients in the TMA cohort were classified into high (n=84) and low (n=240) CDK12 expression groups based on the median IHC score (*Figure 2E*). Additionally, elevated levels of CDK12 correlated with worse OS and disease-free survival (DFS), underscoring a heightened risk of recurrence (*Figure 2F*). The results suggest that the amplification of CDK12 is correlated with both a poor prognosis and tumor recurrence.

OXA efficacy is enhanced by CDK12 inhibition in vitro

To investigate the potential link between CDK12 expression and chemoresistance in GC, we examined the relationship between CDK12 expression levels and OXA-induced cytotoxicity across a panel of GC cell lines (*Figure 3A*). The colony formation assay results showed that CDK12 overexpression decreased OXA-induced apoptosis (*Figure 3B*). We then investigated the effect of CDK12 inhibition on the cell viability-suppressing effect of OXA. The proliferation and colony formation assay results revealed that combining the CDK12 inhibitor THZ531 with OXA significantly potentiated the OXA suppressive effects on cell growth and colony formation (*Figure 3C,3D*). Cancer stemness is associated with enhanced chemoresistance and plays a critical role in tumor recurrence (24,25). Sphere-forming capacity is a widely used *in vitro* method to assess tumor cell stemness. To further investigate the role of CDK12 in regulating stem-like properties in GC, we evaluated the effect of CDK12 inhibition on tumorsphere formation. Notably, the pharmacological inhibition of CDK12 exerted a potent synergistic effect in conjunction with OXA to impede tumorsphere formation (*Figure 3E*). Our results suggest that targeting CDK12 may improve OXA sensitivity in GC.

CDK12 inhibition significantly enhances the anti-tumor effect of OXA in vivo

To further evaluate the therapeutic potential *in vivo*, we assessed the anti-tumor efficacy of OXA and THZ531 in xenograft mouse model. The combination significantly suppressed tumor growth in contrast to monotherapy or the control group as indicated by decrease in both the tumor dimensions and mass (*Figure 4A*). Importantly, the combination regimen was well tolerated, with no significant body weight loss observed in any group throughout the study (*Figure 4B*). Additionally, the tumor volume measurements revealed a significant decrease in the combination group relative to the OXA-only or THZ531-only groups (*Figure 4C*). The statistical analysis further confirmed a synergistic effect, with tumor weights significantly lower in the combination group ($P<0.01$, $P<0.001$; *Figure 4D*). Moreover, the IHC analysis showed that the combination treatment produced a more significant anti-tumor effect compared to either treatment alone. This was characterized by a significant decrease in Ki-67 and cleaved-caspase 3 (*Figure 4E-4G*). Collectively, these findings show the enhanced therapeutic efficacy of combining CDK12 inhibition with OXA and highlight its potential clinical value in treating GC patients.

MAPK signaling is involved in GC cell OXA resistance and enhanced DNA damage

To further evaluate the molecular mechanism underlying the synergistic effect of CDK12 inhibition and OXA, we conducted RNA sequencing on NUGC3 cells treated with OXA with or without the CDK12 inhibitor. The KEGG pathway enrichment analysis revealed that hallmark KRAS signaling downregulation (DN) was significantly enriched in the combination group (*Figure 5A*). The GSEA results further supported these findings, showing the activation of KRAS signaling DN in cells receiving the combination therapy (*Figure 5B*). Given the pivotal role of the Ras-

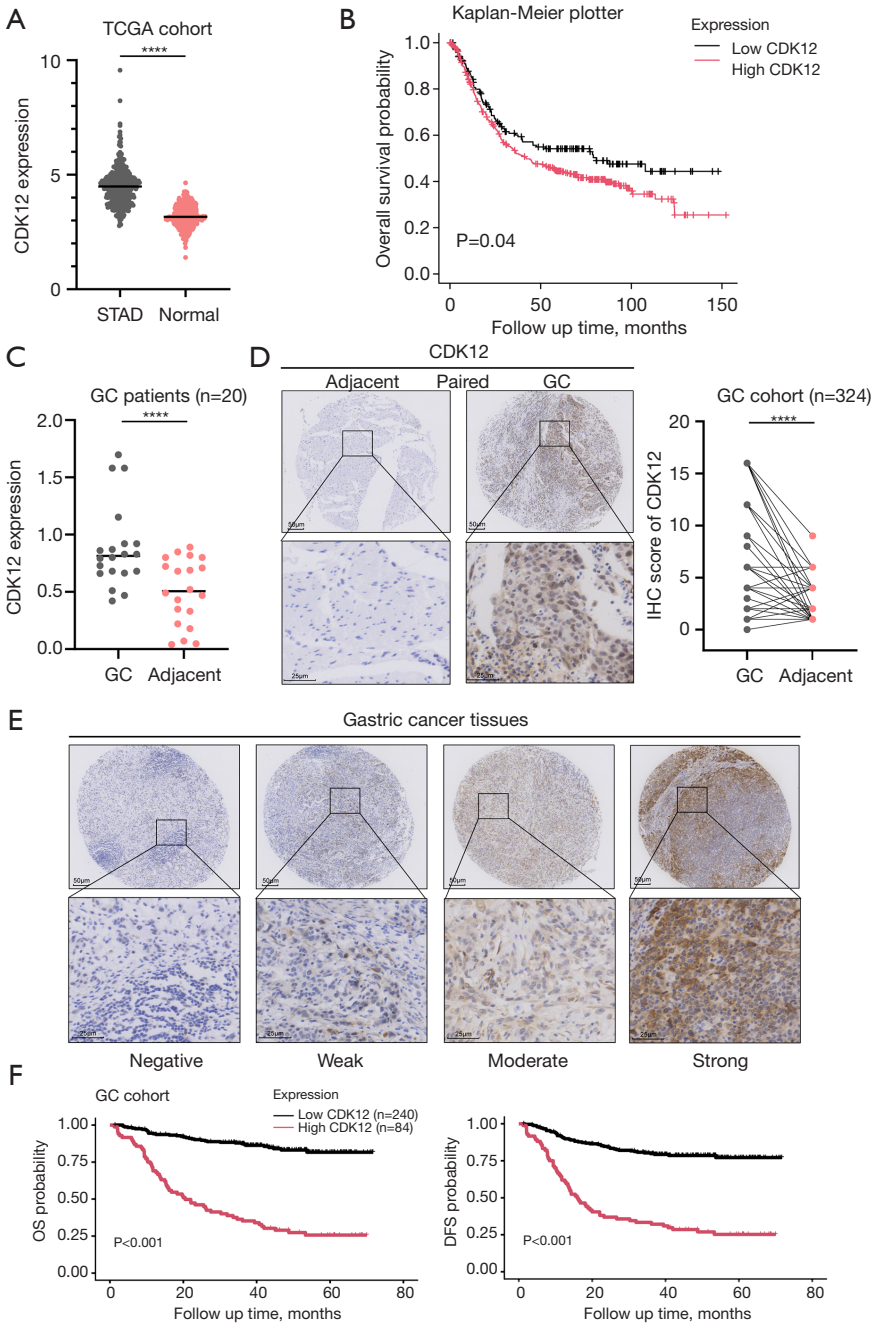

Figure 2 CDK12 is increased in tumor tissues, and is associated with the poor prognosis of GC patients. (A) mRNA expression levels of CDK12 in tumor tissues and normal tissues based on TCGA-STAD cohort. (B) The K-M curves of OS in the GC cohort from the K-M plotter database grouped according to high (red, n=460) and low (black, n=171) CDK12 expression. (C) Reverse transcription-qPCR analysis of CDK12 expression in tumor tissues and adjacent normal tissues. (D) Representative IHC images showing CDK12 expression in GC tissues and normal control tissues from the cohort, and the semi-quantitative analysis of CDK12 IHC staining in paired GC tissues (scale bar: 50 and 25 μm). (E) Representative findings of CDK12 protein expression by IHC, which were graded based on staining intensity in 324 GC tissues (scale bar: 50 and 25 μm). (F) OS and DFS according to CDK12 expression. Student's *t*-test, ****, P<0.0001. CDK12, cyclin-dependent kinase 12; DFS, disease-free survival; GC, gastric cancer; IHC, immunohistochemical; K-M, Kaplan-Meier; OS, overall survival; qPCR, quantitative polymerase chain reaction; STAD, stomach adenocarcinoma; TCGA, The Cancer Genome Atlas.

Table 1 Relationship between CDK12 protein expression levels and clinicopathological characteristics in GC patients

Variables	Overall (n=324), n (%)	Low CDK12 (n=240), n (%)	High CDK12 (n=84), n (%)	P value
Gender				0.99
Female	105 (32.4)	78 (32.5)	27 (32.1)	
Male	219 (67.6)	162 (67.5)	57 (67.9)	
Age (years)				0.008
≤60	146 (45.1)	119 (49.6)	27 (32.1)	
>60	178 (54.9)	121 (50.4)	57 (67.9)	
Differentiation				0.48
High	18 (5.6)	12 (5.0)	6 (7.1)	
Low	235 (72.5)	172 (71.7)	63 (75.0)	
Middle	71 (21.9)	56 (23.3)	15 (17.9)	
Lauren classification				0.50
Diffuse	130 (40.1)	92 (38.3)	38 (45.2)	
Intestinal	105 (32.4)	77 (32.1)	28 (33.3)	
Mixed	81 (25.0)	65 (27.1)	16 (19.0)	
Unknown	8 (2.5)	6 (2.5)	2 (2.4)	
T				0.08
I	40 (12.3)	34 (14.2)	6 (7.1)	
II	39 (12.0)	33 (13.8)	6 (7.1)	
III	216 (66.7)	154 (64.2)	62 (73.8)	
IV	29 (9.0)	19 (7.9)	10 (11.9)	
N				0.02
0	108 (33.3)	89 (37.1)	19 (22.6)	
1	60 (18.5)	46 (19.2)	14 (16.7)	
2	56 (17.3)	42 (17.5)	14 (16.7)	
3	100 (30.9)	63 (26.2)	37 (44.0)	
M				0.005
0	293 (90.4)	224 (93.3)	69 (82.1)	
1	31 (9.6)	16 (6.7)	15 (17.9)	
Stage				0.001
1	57 (17.6)	49 (20.4)	8 (9.5)	
2	108 (33.3)	86 (35.8)	22 (26.2)	
3	128 (39.5)	89 (37.1)	39 (46.4)	
4	31 (9.6)	16 (6.7)	15 (17.9)	
LVI				0.02
No	209 (64.5)	164 (68.3)	45 (53.6)	
Yes	115 (35.5)	76 (31.7)	39 (46.4)	
PNI				0.99
No	197 (60.8)	146 (60.8)	51 (60.7)	
Yes	127 (39.2)	94 (39.2)	33 (39.3)	

CDK12, cyclin-dependent kinase 12; GC, gastric cancer; LVI, lymphovascular invasion; M, metastasis; N, node; T, tumor; PNI, perineural invasion.

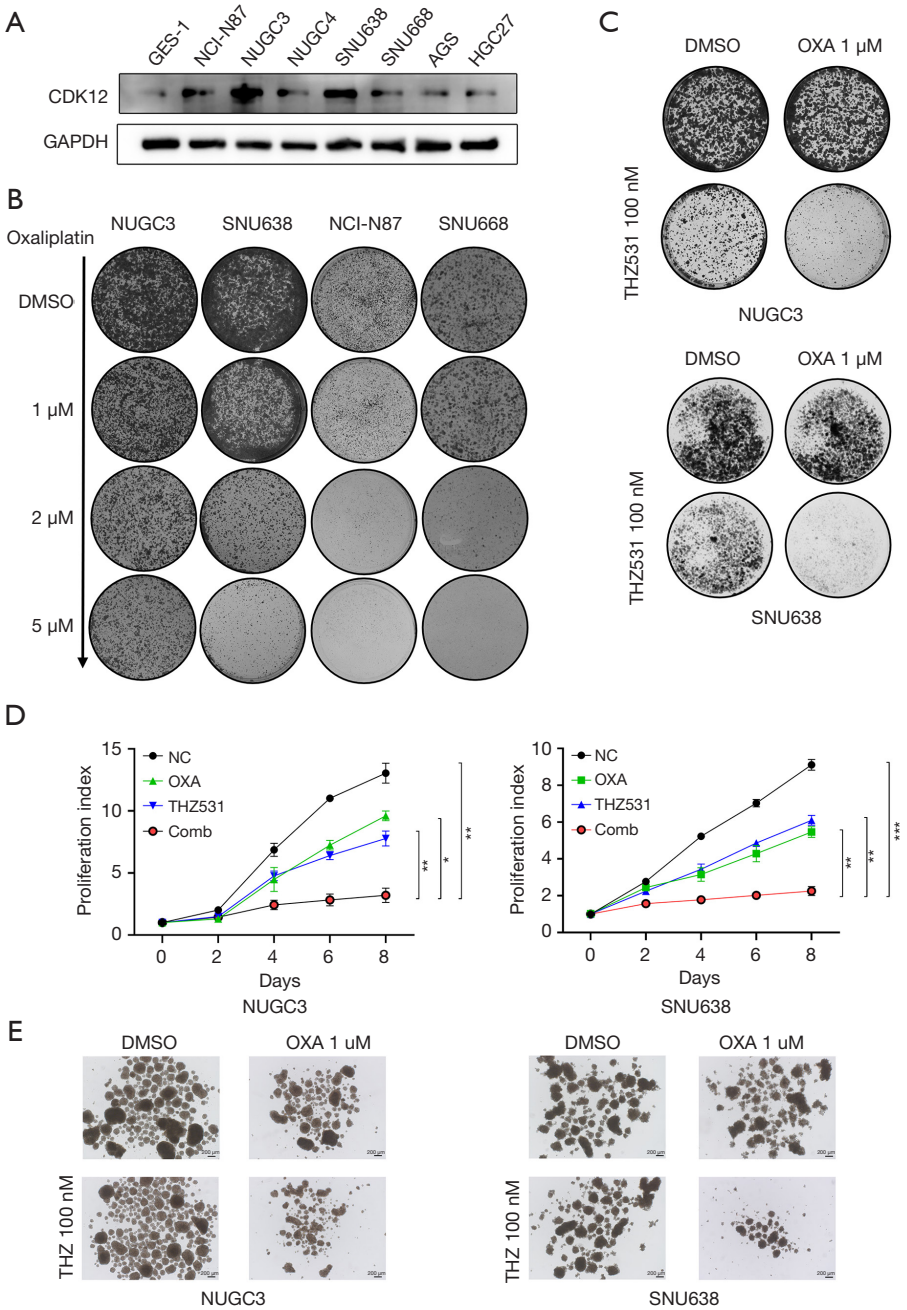

Figure 3 OXA efficacy is enhanced by CDK12 inhibition *in vitro*. (A) CDK12 expression in human gastric cell lines; normal gastric epithelial cells GES-1, and the GC cell lines AGS, NCI-N87, SNU638, SNU668, NUGC3, NUGC4 and HGC27 were evaluated by western blotting. (B) Colony formation assay of high level CDK12 cancer cell lines treated with different dosages of OXA. Colonies were stained with crystal violet. (C) Colony formation assay of cells treated with the CDK12 inhibitor (THZ531), OXA, or a combination of both at 12 days. Colonies were stained with crystal violet. (D) The growth curve of NUGC3 and SNU638 with the CDK12 inhibitor (THZ531, 0.1 μM) combined with OXA (1.0 μM) at the indicated concentration. Data are presented as the mean ± standard deviation. *, P<0.05; **, P<0.01; ***, P<0.001. (E) Representative image of a tumor sphere formation assay of NUGC3 and SNU638 treated with the CDK12 inhibitor (THZ531), OXA, or a combination of these compounds at specified concentrations for a duration of 10 days (scale bar: 200 μm). Tumor spheres were visualized by bright-field microscopy. CDK12, cyclin-dependent kinase 12; DMSO, dimethyl sulfoxide; GAPDH, glyceraldehyde-3-phosphate dehydrogenase; NC, negative control; OXA, oxaliplatin.

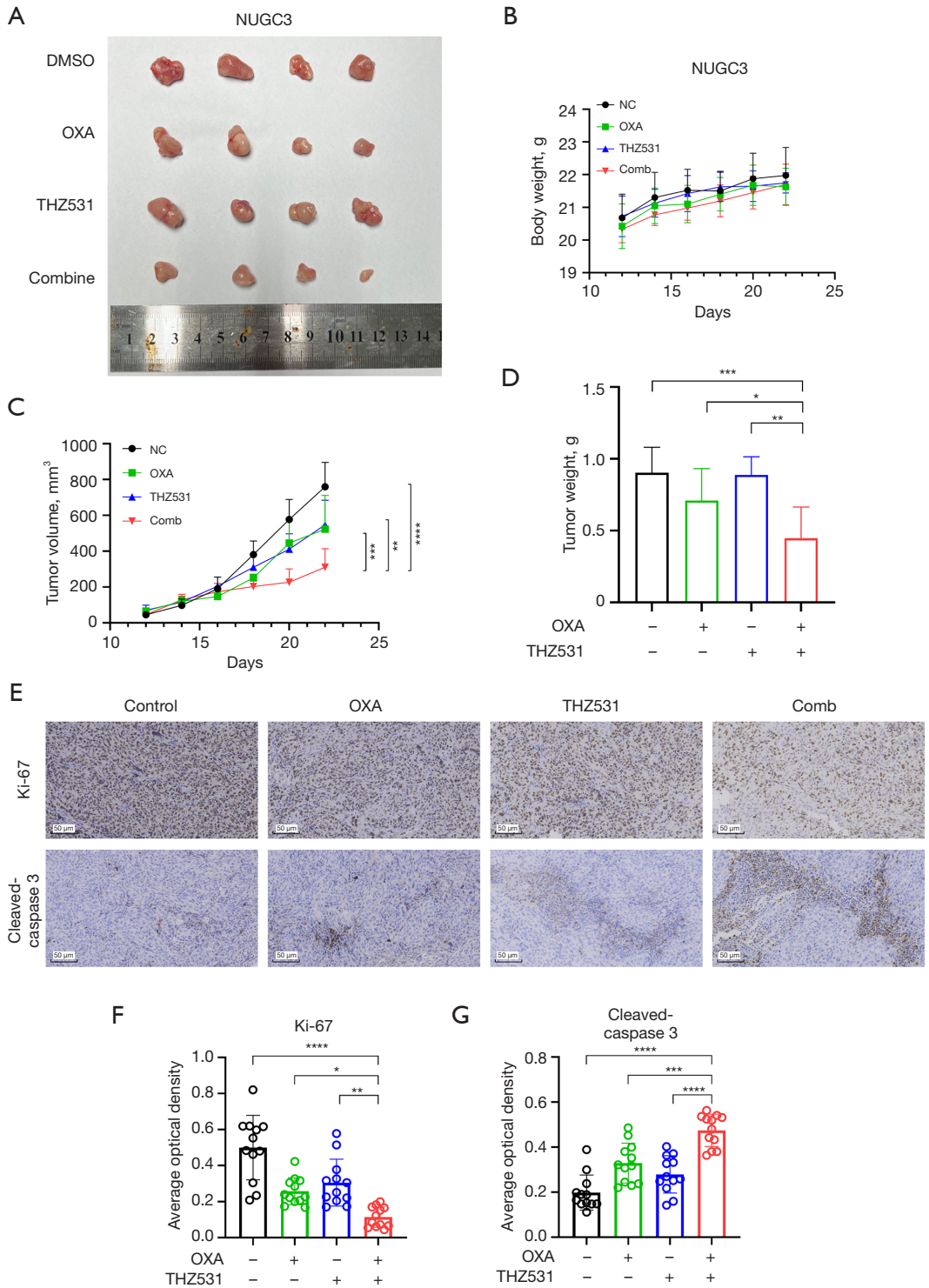

Figure 4 CDK12 inhibition significantly enhances the anti-tumor effect of OXA *in vivo*. (A) Representative tumor images. (B) Body weight. (C) Growth curve of tumor volume. (D) Tumor weight. (E-G) Representative IHC images showing the expression of Ki-67 (F) and cleaved-caspase 3 (G) in NUGC3 xenograft tumors, visualized using DAB chromogenic staining (scale bar: 50 μm). *, P<0.05; **, P<0.01; ***, P<0.001; ****, P<0.0001. CDK12, cyclin-dependent kinase 12; DMSO, dimethyl sulfoxide; IHC, immunohistochemical; NC, negative control; OXA, oxaliplatin.

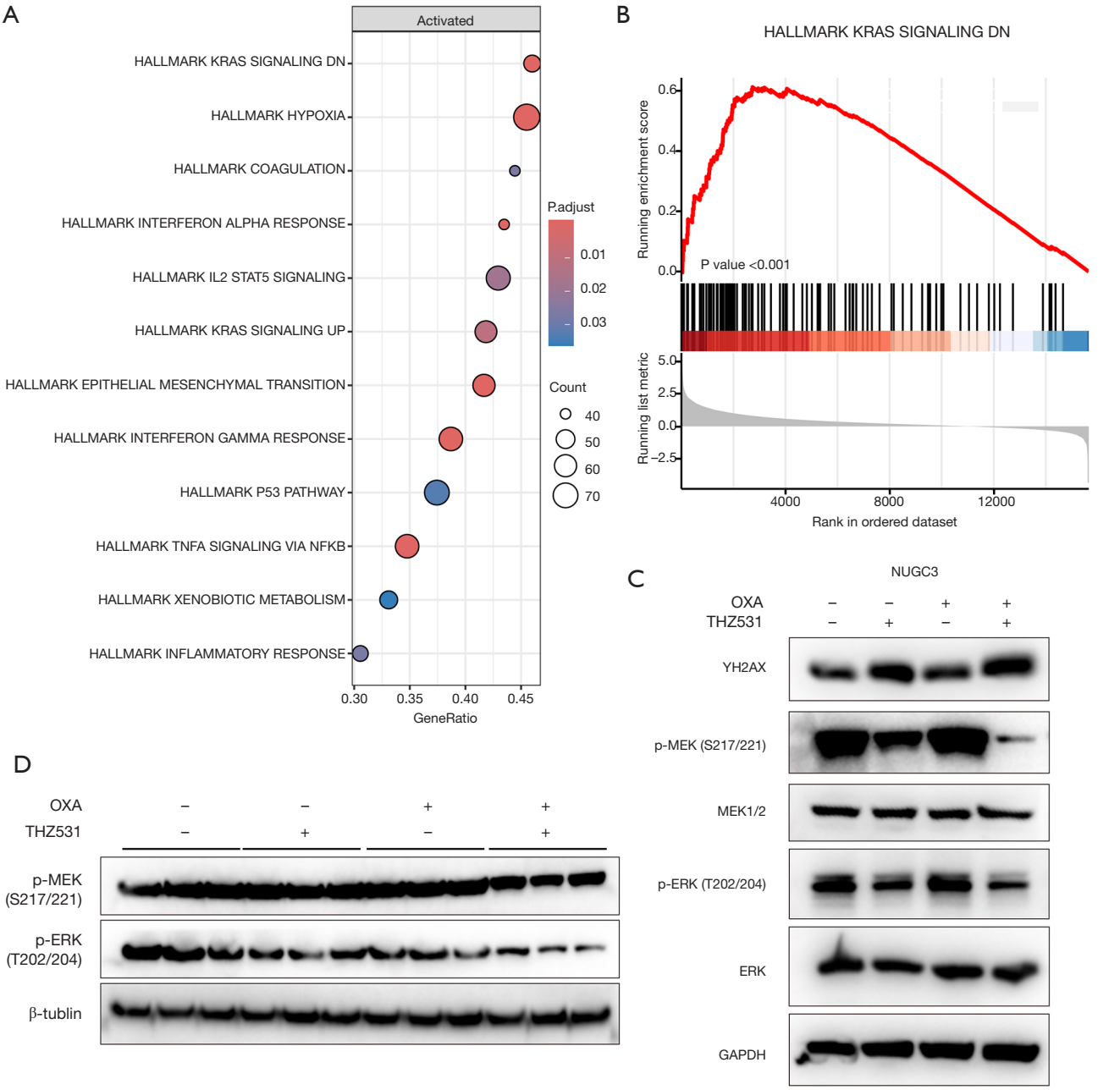

Figure 5 MAPK signaling is involved in GC cell OXA resistance and enhanced DNA damage. (A) Pathway enrichment analysis of RNA-sequencing data revealed the significant activation of various signaling pathways in GC cells after the combined treatment, with the hallmark KRAS signaling downregulation pathway showing the most prominent enrichment (adjusted P value <0.01). (B) GSEA results showing the activation of KRAS signaling downregulation (KRAS signaling DN) in the combined treatment group (OXA + THZ531) compared to the control group as indicated by the elevated running enrichment score (red line) and significant P value (P value <0.001). (C) γH2AX and MAPK signaling pathway analyses by western blotting in the NUGC3 GC cells after treatment with the CDK12 inhibitor THZ531 and OXA. (D) Western blot further confirmed the reduction in MAPK pathway activation (i.e., the phosphorylation of MEK and ERK) following the combined treatment with OXA and THZ531 in the NUGC3 xenografts tumors. CDK12, cyclin-dependent kinase 12; KRAS signaling DN, KRAS signaling downregulation; GAPDH, glyceraldehyde-3-phosphate dehydrogenase; GC, gastric cancer; GSEA, gene set enrichment analysis; OXA, oxaliplatin.

Raf-MEK-ERK signaling cascade in regulating cellular proliferation, differentiation, and survival (26,27), we next investigated whether CDK12 inhibition enhances OXA sensitivity by blocking the activation of the MAPK signaling pathway. It was observed that the phosphorylation levels of MEK and ERK were significantly suppressed in the context of OXA or THZ531 monotherapy, with a more pronounced effect in the combination therapy group (*Figure 5C*). Additionally, the γ-H2AX levels were significantly elevated in the combination group, indicating increased DNA damage when CDK12 inhibitor was combined with OXA (*Figure 5C*). The outcomes were congruent with our hypothesis, suggesting that the combination of OXA and CDK12 inhibitor further downregulate the MAPK signaling pathway. This phenomenon was further confirmed in the NUGC3-derived xenograft mouse model where the combination therapy resulted in a dramatic suppression of the MAPK signaling pathway compared to the control or monotherapy groups (*Figure 5D*). Collectively, the pharmacological inhibition of CDK12 disrupts this pathway, amplifies OXA-induced DNA damage, and ultimately enhances anti-tumor efficacy. These findings highlight the therapeutic potential of targeting CDK12 to overcome OXA resistance in GC.

Discussion

Chemotherapy based on OXA continues to be the standard treatment for GC; however, resistance can lead to treatment failure and poorer outcome. In this study, we showed that CDK12 is frequently amplified and overexpressed in GC tissues and it correlates with poor OS and DFS. Functionally, THZ531, a CDK12 inhibitor, significantly sensitized the GC cells to OXA *in vitro* and *in vivo* by enhancing DNA damage and apoptosis. Mechanistically, CDK12-driven resistance is mediated by the activation of the MAPK signaling pathway (*Figure 6*). These findings establish CDK12 as a promising therapeutic target for overcoming chemoresistance and improving clinical outcomes in GC.

Disruption of the cell cycle is a hallmark of cancer progression and treatment resistance (28). CDKs, as master regulators of cell-cycle progression and transcriptional control, have emerged as attractive therapeutic targets across various malignancies (29-31). Among them, CDK12 has been shown to play a pivotal role in maintaining genomic stability by regulating the transcription of DNA damage response genes, and its silencing is lethal in cancers like breast cancer and osteosarcoma (18,32). Studies have reported that CDK12 plays a significant role in the biological processes of GC, but this remains a subject of debate. One study reported reduced CDK12 expression in GC tissues (33), while other investigations have identified CDK12 as an oncogenic driver that promotes tumor progression (34,35). The variations in results might be due to the different age groups and limited sample sizes. Our data supported the latter finding; that is, our MR analysis revealed a causal association between elevated CDK12 expression and increased GC risk, underscoring its potential role in disease initiation and progression. Consistently, both the qPCR and IHC analyses confirmed significantly higher CDK12 expression in GC tissues compared to adjacent non-tumorous tissues. Together, these findings support the notion that CDK12 acts as an oncogenic driver in GC, and highlight its potential as a promising therapeutic target for overcoming disease progression and resistance.

Additionally, there is increasing evidence showing the effectiveness of CDK12 inhibition in inhibiting tumor proliferation, and synthetic-lethal interactions have been described with targeted therapeutics (36). Johnson and colleagues showed that the pharmacological inhibition of CDK12 significantly enhanced the sensitivity of breast cancer cells to poly(ADP-ribose) polymerase (PARP) inhibitors, promoting synthetic-lethality through homologous recombination (HR) deficiency (18). In parallel, Choi *et al.* reported that CDK12 inhibition potentiates the anti-tumor efficacy of trastuzumab in HER2-positive breast cancer (37). Moreover, Maity *et al.*'s study provided compelling evidence that targeting CDK12 can reverse acquired resistance to osimertinib in lung adenocarcinoma (38). While these findings have been well documented in breast, lung, and prostate cancers, their relevance in GC remains incompletely understood.

Our work extends the concept of CDK12 inhibition-mediated chemosensitization to GC, linking CDK12's DNA repair function to the OXA chemotherapeutic response. Our study showed that CDK12 inhibition significantly enhanced the efficacy of OXA against GC cells. Compared to OXA treatment alone, treating the cells with the CDK12 inhibitor led to increased OXA-induced DNA damage and apoptosis. We also observed higher levels of γH2A and cleaved-caspase 3 in the CDK12-suppressed cells upon OXA exposure. These results indicated that the CDK12-inhibited cells could not effectively repair or tolerate the DNA lesions from OXA, resulting in the accumulation of lethal damage.

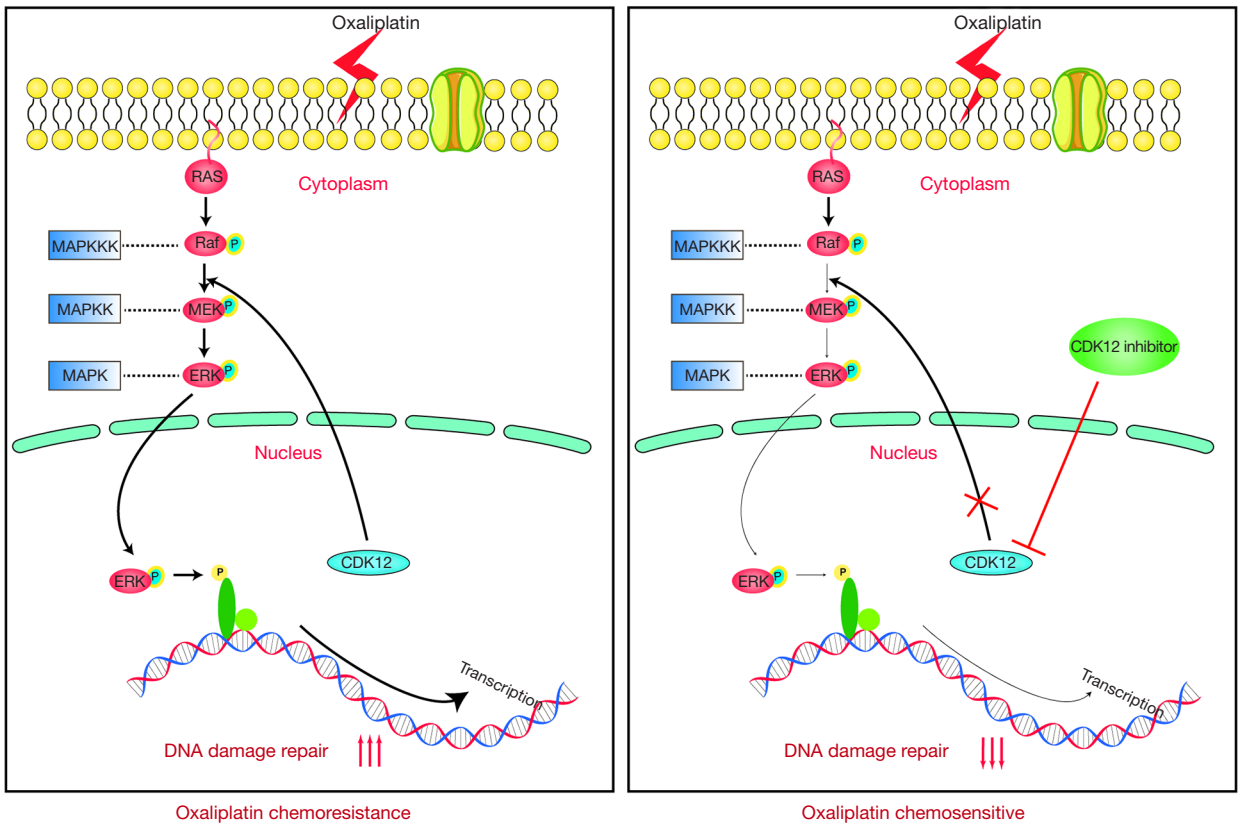

Figure 6 Schematic model illustrating the role of CDK12 in mediating OXA resistance in GC via the activation of the MAPK signaling pathway. CDK12 overexpression activates the MAPK signaling pathway, leading to enhanced DNA damage repair and reduced sensitivity to OXA in GC. The pharmacological inhibition of CDK12 significantly suppresses MAPK pathway phosphorylation, thereby impairing DNA repair mechanisms and amplifying OXA-induced DNA damage. Targeting CDK12 may serve as a promising therapeutic strategy for overcoming chemoresistance and improve the clinical outcomes of OXA-based chemotherapy in GC. CDK12, cyclin-dependent kinase 12; GC, gastric cancer; OXA, oxaliplatin.

Several studies tried to explore the mechanism of CDK12 inhibition in overcoming drug resistance; for instance, Choi *et al.* reported that CDK12 inhibition potentiates the anti-tumor efficacy of trastuzumab in HER2-positive breast cancer and Maity *et al.* showed that targeting CDK12 reverses resistance to osimertinib in lung adenocarcinoma via the inhibition of the AKT signaling pathway (37,38). In relation to GC, our findings indicated that the inhibition of CDK12 enhances the therapeutic efficacy of OXA by disrupting MAPK signaling. The MAPK cascade governs critical cellular processes, such as proliferation and survival, and may contribute to chemoresistance. We showed that CDK12 inhibition attenuates the phosphorylation of key MAPK components, MEK and ERK, and potentiates OXA-induced DNA damage, offering a mechanistic basis for the observed synergy.

Our research provides significant insights into the function of CDK12 in GC; however, some limitations merit consideration. Despite the efficacy observed with THZ531 in preclinical models, it exhibits dual inhibitory activity against both CDK12 and CDK13 due to the high degree of structural homology between these kinases (39,40). Thus, highly selective CDK12 inhibitors need to be developed to mitigate these risks and maximize the clinical benefits. Further, the conclusions drawn from our study are based on *in vitro* and *in vivo* preclinical models. The translational potential of CDK12 inhibition in GC requires rigorous evaluation in clinical settings to assess its safety, pharmacodynamics, and therapeutic efficacy.

Therapeutically, these findings have important implications. OXA induces extensive DNA crosslinks and double-strand breaks, while CDK12 inhibition cripples

the transcriptional regulation of DNA damage repair genes, specifically impairing HR repair. Together, this dual blockade overwhelms the tumor capacity to repair genomic lesions, leading to restored chemosensitivity in GC cells. These observations suggest that co-targeting CDK12 alongside DNA-damaging agents like OXA could represent a compelling strategy for overcoming chemoresistance in refractory GC.

Conclusions

This study identified CDK12 as a critical regulator of chemoresistance in GC and highlighted its potential as a therapeutic target. By combining CDK12 inhibition with OXA, we offer a novel strategy for overcoming chemotherapy resistance, improving treatment efficacy, and ultimately enhancing the clinical outcomes of patients with advanced GC.

Acknowledgments

The authors would like to thank Dr. Huaxian Chen from Sun Yat-sen University for providing critical comments and advice on the manuscript. The authors would also like to express their gratitude to all the patients who generously contributed samples to this study.

Footnote

Reporting Checklist: The authors have completed the ARRIVE and MDAR reporting checklists. Available at https://jgo.amegroups.com/article/view/10.21037/jgo-2025-392/rc

Data Sharing Statement: Available at https://jgo.amegroups.com/article/view/10.21037/jgo-2025-392/dss

Peer Review File: Available at https://jgo.amegroups.com/article/view/10.21037/jgo-2025-392/prf

Funding: This study was supported by the National Natural Science Foundation of China (No. 82070684) and the Guangzhou Science and Technology Plan Project: 2025 Special Program on Basic and Applied Basic Research (Outstanding Doctoral "Continuation" Project, No. 2025A04J5296).

Conflicts of Interest: All authors have completed the ICMJE uniform disclosure form (available at https://jgo.amegroups.com/article/view/10.21037/jgo-2025-392/coif). The authors have no conflicts of interest to declare.

Ethical Statement: The authors are accountable for all aspects of the work in ensuring that questions related to the accuracy or integrity of any part of the work are appropriately investigated and resolved. The study was conducted in accordance with the Declaration of Helsinki and its subsequent amendments. The study was approved by the Research Ethics Board at The Sixth Affiliated Hospital of Sun Yat-sen University (No. 2025ZSLYEC-047) and informed consent was taken from all the patients. Animal Experiments were performed under a project license (No. IACUC-2023080302) granted by the Laboratory Animal Ethics Committee of The Sixth Affiliated Hospital of Sun Yat-sen University, in compliance with institutional guidelines for the care and use of animals.

References

1. Bray F, Laversanne M, Sung H, et al. Global cancer statistics 2022: GLOBOCAN estimates of incidence and mortality worldwide for 36 cancers in 185 countries. CA Cancer J Clin 2024;74:229-63.
2. Zheng RS, Chen R, Han BF, et al. Cancer incidence and mortality in China, 2022. Zhonghua Zhong Liu Za Zhi 2024;46:221-31.
3. Siegel R, Naishadham D, Jemal A. Cancer statistics, 2013. CA Cancer J Clin 2013;63:11-30.
4. Kawai S, Fukuda N, Yamamoto S, et al. Retrospective observational study of salvage line ramucirumab monotherapy for patients with advanced gastric cancer. BMC Cancer 2020;20:338.
5. Zhang F, Wang H, Yu J, et al. LncRNA CRNDE attenuates chemoresistance in gastric cancer via SRSF6-regulated alternative splicing of PICALM. Mol Cancer 2021;20:6.

6. Xu Y, Zhao Y, Guo X, et al. Plasma metabolic profiling analysis of neurotoxicity induced by oxaliplatin using metabonomics and multivariate data analysis. Toxicol Res (Camb) 2018;7:529-37.
7. Chen HY, Islam A, Yuan TM, et al. Regulation of tNOX expression through the ROS-p53-POU3F2 axis contributes to cellular responses against oxaliplatin in human colon cancer cells. J Exp Clin Cancer Res 2018;37:161.
8. Hanahan D, Weinberg RA. Hallmarks of cancer: the next generation. Cell 2011;144:646-74.
9. Ding L, Yang L, He Y, et al. CREPT/RPRD1B associates with Aurora B to regulate Cyclin B1 expression for accelerating the G2/M transition in gastric cancer. Cell Death Dis 2018;9:1172.
10. Houles T, Lavoie G, Nourreddine S, et al. CDK12 is hyperactivated and a synthetic-lethal target in BRAF-mutated melanoma. Nat Commun 2022;13:6457.
11. Wu YM, Cieślik M, Lonigro RJ, et al. Inactivation of CDK12 Delineates a Distinct Immunogenic Class of Advanced Prostate Cancer. Cell 2018;173:1770-1782.e14.
12. Quereda V, Bayle S, Vena F, et al. Therapeutic Targeting of CDK12/CDK13 in Triple-Negative Breast Cancer. Cancer Cell 2019;36:545-558.e7.
13. Chou J, Quigley DA, Robinson TM, et al. Transcription-Associated Cyclin-Dependent Kinases as Targets and Biomarkers for Cancer Therapy. Cancer Discov 2020;10:351-70.
14. Vervoort SJ, Welsh SA, Devlin JR, et al. The PP2A-Integrator-CDK9 axis fine-tunes transcription and can be targeted therapeutically in cancer. Cell 2021;184:3143-3162.e32.
15. Tang R, Liu J, Li S, et al. A patent and literature review of CDK12 inhibitors. Expert Opin Ther Pat 2022;32:1055-65.
16. He Y, Xu W, Xiao YT, et al. Targeting signaling pathways in prostate cancer: mechanisms and clinical trials. Signal Transduct Target Ther 2022;7:198.
17. Dubbury SJ, Boutz PL, Sharp PA. CDK12 regulates DNA repair genes by suppressing intronic polyadenylation. Nature 2018;564:141-5.
18. Johnson SF, Cruz C, Greifenberg AK, et al. CDK12 Inhibition Reverses De Novo and Acquired PARP Inhibitor Resistance in BRCA Wild-Type and Mutated Models of Triple-Negative Breast Cancer. Cell Rep 2016;17:2367-81.
19. Luo D, Wang H, Liu J, et al. Combined MDM2 and G2/M checkpoint inhibition induces synergistic antitumor response in gastric signet-ring cell carcinoma. Cancer Lett 2025;613:217500.
20. Rebhan M, Chalifa-Caspi V, Prilusky J, et al. GeneCards: a novel functional genomics compendium with automated data mining and query reformulation support. Bioinformatics 1998;14:656-64.
21. Malumbres M, Harlow E, Hunt T, et al. Cyclin-dependent kinases: a family portrait. Nat Cell Biol 2009;11:1275-6.
22. Malumbres M. Cyclin-dependent kinases. Genome Biol 2014;15:122.
23. Bertoli C, Skotheim JM, de Bruin RA. Control of cell cycle transcription during G1 and S phases. Nat Rev Mol Cell Biol 2013;14:518-28.
24. Lee KM, Giltnane JM, Balko JM, et al. MYC and MCL1 Cooperatively Promote Chemotherapy-Resistant Breast Cancer Stem Cells via Regulation of Mitochondrial Oxidative Phosphorylation. Cell Metab 2017;26:633-647.e7.
25. Ye H, Adane B, Khan N, et al. Leukemic Stem Cells Evade Chemotherapy by Metabolic Adaptation to an Adipose Tissue Niche. Cell Stem Cell 2016;19:23-37.
26. McCubrey JA, Steelman LS, Chappell WH, et al. Roles of the Raf/MEK/ERK pathway in cell growth, malignant transformation and drug resistance. Biochim Biophys Acta 2007;1773:1263-84.
27. Chang F, Steelman LS, Shelton JG, et al. Regulation of cell cycle progression and apoptosis by the Ras/Raf/MEK/ERK pathway (Review). Int J Oncol 2003;22:469-80.
28. Liu J, Peng Y, Wei W. Cell cycle on the crossroad of tumorigenesis and cancer therapy. Trends Cell Biol 2022;32:30-44.
29. Łukasik P, Załuski M, Gutowska I. Cyclin-Dependent Kinases (CDK) and Their Role in Diseases Development-Review. Int J Mol Sci 2021;22:2935.
30. Ghafouri-Fard S, Khoshbakht T, Hussen BM, et al. A review on the role of cyclin dependent kinases in cancers. Cancer Cell Int 2022;22:325.
31. Knudsen ES, Kumarasamy V, Nambiar R, et al. CDK/cyclin dependencies define extreme cancer cell-cycle heterogeneity and collateral vulnerabilities. Cell Rep 2022;38:110448.
32. Bayles I, Krajewska M, Pontius WD, et al. Ex vivo screen identifies CDK12 as a metastatic vulnerability in osteosarcoma. J Clin Invest 2019;129:4377-92.
33. Liu M, Fan H, Li T, et al. Low expression of CDK12 in gastric cancer is correlated with advanced stage and poor outcome. Pathol Res Pract 2020;216:152962.
34. Liu H, Shin SH, Chen H, et al. CDK12 and PAK2 as novel therapeutic targets for human gastric cancer.

Theranostics 2020;10:6201-15.
35. Gao LZ, Wang JQ, Chen JL, et al. CDK12 Promotes the Proliferation, Migration, and Angiogenesis of Gastric Carcinoma via Activating the PI3K/AKT/mTOR Signaling Pathway. Appl Biochem Biotechnol 2023;195:6913-26.
36. Wang C, Wang H, Lieftink C, et al. CDK12 inhibition mediates DNA damage and is synergistic with sorafenib treatment in hepatocellular carcinoma. Gut 2020;69:727-36.
37. Choi HJ, Jin S, Cho H, et al. CDK12 drives breast tumor initiation and trastuzumab resistance via WNT and IRS1-ErbB-PI3K signaling. EMBO Rep 2019;20:e48058.
38. Maity TK, Kim EY, Cultraro CM, et al. Novel CDK12/13 Inhibitors AU-15506 and AU-16770 Are Potent Anti-Cancer Agents in EGFR Mutant Lung Adenocarcinoma with and without Osimertinib Resistance. Cancers (Basel) 2023;15:2263.
39. Jiang B, Gao Y, Che J, et al. Discovery and resistance mechanism of a selective CDK12 degrader. Nat Chem Biol 2021;17:675-83.
40. Zhang T, Kwiatkowski N, Olson CM, et al. Covalent targeting of remote cysteine residues to develop CDK12 and CDK13 inhibitors. Nat Chem Biol 2016;12:876-84.

Cite this article as: Huang D, Xiong Z, Zhong B, Li X, Mohamed SA, Sun J, Xu H, Guo J, Deng Z, Li X, Almhanna K, Chen Y, Lian L. CDK12 inhibition enhances oxaliplatin efficacy in gastric cancer by suppressing the MAPK signaling pathway. J Gastrointest Oncol 2025;16(3):823-839. doi: 10.21037/jgo-2025-392